Journal of Power Sources 196 (2011) 1090–1096

Contents lists available at ScienceDirect

Journal of Power Sources

journal homepage: www.elsevier.com/locate/jpowsour

Pt_xSn/C electrocatalysts synthesized by improved microemulsion method and their catalytic activity for ethanol oxidation

Lirong Li, Meihua Huang, Jinjie Liu, Yonglang Guo*

College of Chemistry and Chemical Engineering, Fuzhou University, Fuzhou 350108, PR China

ARTICLE INFO

Article history:
Received 30 June 2010
Received in revised form 10 August 2010
Accepted 10 August 2010
Available online 17 August 2010

Keywords:
Direct ethanol fuel cell
Platinum–tin electrocatalysts
Ethanol oxidation
Microemulsion method

ABSTRACT

The Pt_xSn/C (x = 1, 2, 2.5, 3, 4) anodic catalysts for direct ethanol fuel cell (DEFC) have been prepared by an improved microemulsion method. Ethylene glycol is used as cosurfactant, and metal precursors are dissolved in it beforehand to prevent the hydrolysis of metal precursors. The composition, particle size and structure of these catalysts are characterized by energy dispersive X-ray spectrum (EDX), transmission electron microscope (TEM) and X-ray diffraction (XRD). The results show that the synthesized Pt_3Sn/C catalyst has part of Pt and Sn alloying. The average diameter is about 2.9 nm, and has a narrow size distribution and a good dispersivity. The electrochemical experiments indicate that the Pt_3Sn/C catalyst prepared in the neutral microemulsion has superior catalytic activity for ethanol oxidation. The Pt_xSn/C nanoparticle formation in the improved microemulsion is also discussed.

1. Introduction

In recent years, considerable attention has been paid to the research of the direct methanol fuel cell (DMFC) and direct ethanol fuel cell (DEFC) [1–3]. However, the application of DMFC is greatly limited because methanol is toxic and its crossover through the membrane can reduce the efficiency [4–7]. Ethanol is one of the most attractive fuels among the small organic molecules due to its renewable, abundant availability, low toxicity and high energy density [8,9]. Lamy et al. [10] observed that the characteristics of current density *vs.* cell potential for a proton exchange membrane fuel cell (PEMFC) fed with methanol or ethanol are rather similar at high temperatures. It indicates that ethanol appears as an alternative fuel to methanol. Consequently, DEFC is of increasing importance in the area of fuel cell. However, the complete oxidation of ethanol to CO_2 is more difficult than that of methanol due to the difficulties in C–C bond breaking and the formation of CO-like intermediates that poison the Pt-based anode catalysts [10,11].

Due to the high price and low tolerance to being poisoned by strongly adsorbed species coming from the dissociative adsorption of ethanol, pure platinum is not a suitable electrocatalyst for ethanol anodic reaction when PEMFC is considered as a practical power source [12]. In order to enhance the efficiency and reduce the catalyst price, Pt-based bimetallic or multimetallic catalysts have been widely studied, such as PtRu [13], PtSn [14], PtRh [3], PtMo [15], PtSnPd [12], PtSnNi [16], PtSnRu [17], PtSnRh [18], among which PtRu and PtSn are the most active catalysts of binary alloys. Although PtRu is a best electrocatalyst for the methanol oxidation, its efficiency for ethanol oxidation is lower than that on PtSn [19,20]. Zhou et al. [21,22] prepared various Pt-based catalysts by polyol processes. The results indicate that the electrochemical activity of PtSn is higher than PtRu. Li et al. [23] studied the catalytic activity of PtSn at different potentials and found that PtSn/C has higher performance for ethanol oxidation in the low potential region, while in the high potential region PtRu/C is more active. It is explained that the addition of Sn could induce the extension of Pt–Pt distance and thus enhance the ethanol oxidation at low potential region [23,24]. Compared with platinum, Sn can activate water at lower potentials so that some OH species is formed at low potentials on Sn sites and then the adsorbed acetaldehyde reacts with adsorbed OH species to produce acetic acid [17].

The catalytic activity of PtSn catalyst for ethanol oxidation varies considerably depending on the Pt:Sn molar ratio, the support, and its synthesis [25–27]. The preparation method of PtSn as anodic catalyst has attracted much interest, such as ethylene glycol (EG) or formic acid as reductant [28,29], electrodeposition [30], microwave irradiation [31] and microemulsion [27] methods. Since Boutonnet et al. [32] synthesized metal nanoparticles (Pt, Pd, Rh and Ir) successfully by using water-in-oil microemulsions, the new technique of preparing nanoparticles has been widely employed. Xiong and Manthiram [33] reported that the particle size of the PtFe/C catalyst prepared by microemulsion method was 2.5 nm. Siné et al. [27] synthesized Pt_xSn nanoparticles in water-in-oil (W/O) microemulsion of water/tetraethylene glycol-monododecylether (BRIJ® 30)/*n*-heptane, and then Pt_xSn nanoparticles were deposited on a boron-doped diamond (BDD)

* Corresponding author. Tel.: +86 591 8807 3608; fax: +86 591 8807 3608.
E-mail address: yguo@fzu.edu.cn (Y. Guo).

0378-7753/$ – see front matter © 2010 Elsevier B.V. All rights reserved.
doi:10.1016/j.jpowsour.2010.08.016

substrate electrode. It was observed that the Pt_xSn electrocatalyst with Pt:Sn molar ratio of 80:20 was more active than the catalysts with other ratios in 0.1 M C_2H_5OH + 1 M $HClO_4$ solution.

The nanoparticle synthesizing steps of the conventional microemulsion method are as follows. Metal precursors were dissolved in the aqueous phase, then mixed the aqueous solution with surfactant, cosurfactant and oil to form microemulsion. After that, the reductant was added directly to the system or solubilized into the same microemulsion in the first instance and then added to the system. In this process, water can be solubilized to form water droplets which were delimited by the surfactant and cosurfactant. Consequently, the synthesis reactions took place in these "water droplets" [27,32,33].

Some reactants such as $SnCl_2$ are easy to be hydrolyzed in the water. In order to inhibit this process, it is necessary that the aqueous solution containing reactants should be acidified. In this process, however, some microemulsion systems are sensitive to acid. In this work, the microemulsion synthesis was improved by dissolving metal precursors into ethylene glycol firstly to inhibit hydrolysis of the reactant and keep the neutral aqueous phase. And ethylene glycol is also as a cosurfactant in microemulsion. The Pt_xSn/C catalysts with different atomic ratios of Pt:Sn were synthesized by the improved microemulsion method. Their catalytic activity for the ethanol electro-oxidation was evaluated by electrochemical methods.

2. Experimental

$H_2PtCl_6{\cdot}6H_2O$ and $SnCl_2{\cdot}2H_2O$ with 3:1 atomic ratio of Pt to Sn were dissolved in ethylene glycol (EG), and then double-distilled water, Triton X-100 (t-octyphenoxypolyethoxyethanal) and cyclohexane were added in sequence. The above solution was stirred and ultrasonically dispersed to form a clear water-in-oil microemulsion. The microemulsion consisted of (by volume) 22% Triton X-100 as a surfactant, 11% ethylene glycol (containing Pt–Sn precursor) as a cosurfactant, 63% cyclohexane as the continuous oil phase and 4% double-distilled water as the aqueous phase. Then the Vulcan XC-72R carbon powder was ultrasonically suspended in the microemulsion. Formic acid and sodium hydroxide were mixed at equal molar ratio and they serve as the reductant. Excessive reductant solution (4% volume of the microemulsion) was added dropwise to the microemulsion, followed by agitating for 20 h in N_2 atmosphere at room temperature. Pt_3Sn/C powder samples were obtained by separating and washing the deposition with acetone and double-distilled water for several times. Finally the samples were dried at 80 °C for 3 h in a vacuum oven. With the same procedures, the Pt_4Sn/C, $Pt_{2.5}Sn/C$, Pt_2Sn/C and Pt_1Sn/C were synthesized. The Pt loading of all catalysts was always 20 wt.%.

The ultraviolet spectra was performed on T6 ultraviolet–visible spectrophotometer (UVS). The scan range was from 200 to 400 nm and the bandwidth is 0.1 nm. The atomic ratios of the PtSn/C catalysts were determined by energy dispersive X-ray spectrum (EDX) coupled to Philips-FEI XL30 ESEM-TMP scanning electron microscope (SEM), whose resolution power is 129 eV. The catalyst appearance and particle size were observed by JEOL JEM-1010 transmission electron microscope (TEM) working at 200 kV. X-ray diffraction (XRD) of the catalysts was carried out by Philip X'Pert Pro MPP X-ray powder diffractometer using a Cu Kα radiation (λ = 0.154 nm) at a scan rate of 2° min^{-1}. The scan range was from 20° to 90°.

5 mg catalyst and 1 mL isopropanol were added to 15 μL 15 wt.% Nafion® solution. The mixture was ultrasonically dispersed for 20 min. Then 25 μL catalyst ink was transferred to the glassy carbon disk electrode (diameter 4 mm) and the electrode was dried under an infrared lamp. The Pt loading on glassy carbon electrode

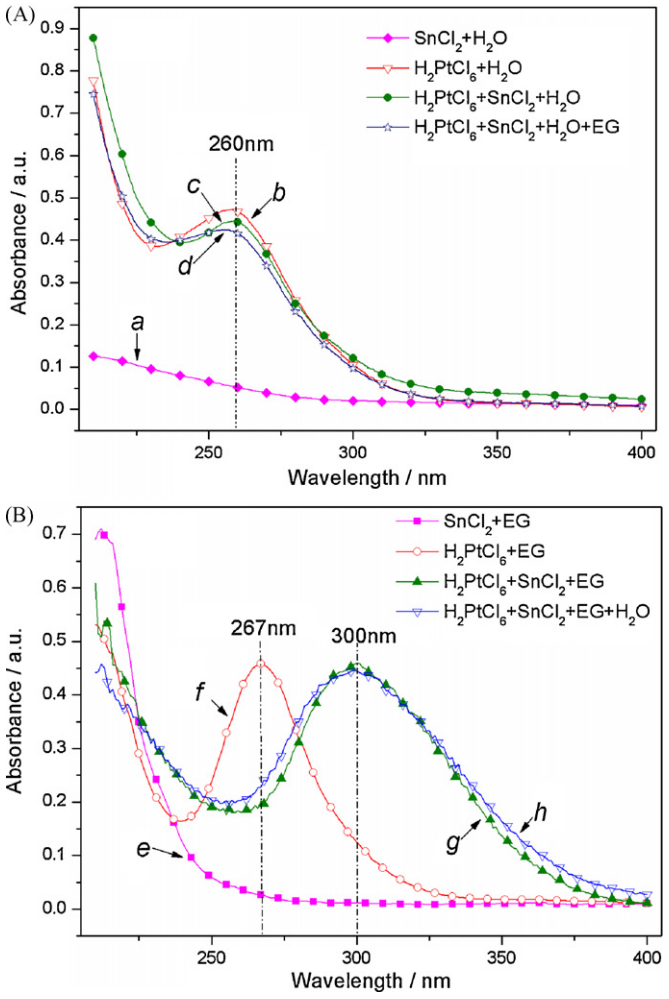

Fig. 1. UV–vis spectra of metal precursors in different solvents. (A) Water; (B) ethylene glycol.

was 0.2 mg cm^{-2}. The electrochemical performance was measured in the electrolyte cell, which was composed of three compartments with Pt foil as counter electrode and Hg/Hg_2SO_4/0.5 M H_2SO_4 (MMS) as reference electrode. Before experiments, the 0.5 M H_2SO_4 + 1.0 M C_2H_5OH or 0.5 M H_2SO_4 solutions were purged with ultrapure nitrogen gas for 20 min to expel oxygen. The electrochemical experiments were carried out on CHI 1140A electrochemical working station at 25 °C.

3. Results and discussion

3.1. Precursor states in different solvents

Fig. 1 shows the UV–vis spectra of metal precursors in different solutions. It can be seen that there is no peak on curve *a* ($SnCl_2 + H_2O$) in Fig. 1A. And there exists a prominent absorption peak at 260 nm on curve *b* ($H_2PtCl_6 + H_2O$), which is attributed to the absorption of Pt^{4+} ions in water [34]. On curve *c*, the absorption peak does not shift in the aqueous solution of H_2PtCl_6 and $SnCl_2$. It indicates that the addition of $SnCl_2$ has no effect on the Pt^{4+} ions in water. The peak also hardly changes when ethylene glycol was put into the aqueous solution of H_2PtCl_6 and $SnCl_2$ (curve *d*). It implies that H_2PtCl_6 and $SnCl_2$ could not form the complex in aqueous solutions even adding ethylene glycol later.

In order to study the effect of the solvent on the metal precursor states, the ethylene glycol was substituted for the hydrosolvent

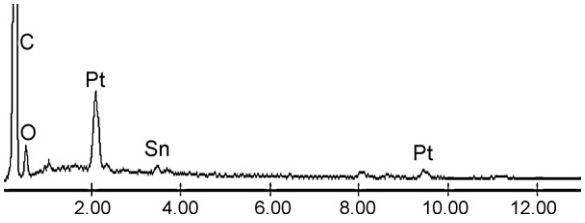

Fig. 2. EDX spectrum of Pt_3Sn/C catalyst.

above. Curve *e* in Fig. 1B shows the UV–vis spectra of $SnCl_2$ dissolved in ethylene glycol. There is no peak between 210 and 400 nm. On curve *f* in H_2PtCl_6 + EG solution, however, there exists a prominent absorption peak at 267 nm. It is also attributed to the absorption of Pt^{4+} ions [35]. So the absorption peak of Pt^{4+} in ethylene glycol is red-shifted, compared with that in aqueous solution (curve *b*). It is ascribed to the solvent effect of ethylene glycol. The absorption peak at 267 nm disappears when H_2PtCl_6, $SnCl_2$ and ethylene glycol are mixed, instead a high absorption peak appears at about 300 nm (curve *g*). Jiang et al. [35] indicated that Pt^{4+} ions reacted with Sn^{2+} ions to form a complex in ethylene glycol system, and their complex structure depends on the Pt:Sn ratios. So the peak at 300 nm is attributed to the complex formed by Pt^{4+} and Sn^{2+} ions in ethylene glycol. In order to research the effect of the hydrosolvent, a certain amount of water is put into the solution above. Curve *h* shows that no change takes place in the absorption peak at 300 nm. Although the solutions of curve *h* and curve *d* are in the same $SnCl_2 + H_2PtCl_6 + EG + H_2O$ system with difference in adding order of solvents, they are quite different. Therefore, Pt^{4+} cannot complex with Sn^{2+} when H_2PtCl_6 and $SnCl_2$ are dissolved in water beforehand, even after adding complex agent of EG. When they are dissolved in EG, however, a complex containing Pt^{4+} and Sn^{2+} ions can be formed and the addition of water does not destroy the Pt–Sn complex in ethylene glycol system. It is deduced that metal precursors of Pt^{4+} and Sn^{2+} ions exist in the form of complex in ethylene glycol. This complex is beneficial to the alloying of Pt and Sn. The metal precursors are first dissolved in ethylene glycol and the ethylene glycol is used as cosurfactant in W/O microemulsion.

3.2. Physical characterization

The composition of the catalyst was evaluated by EDX analysis. Fig. 2 shows the typical EDX spectrum of Pt_3Sn/C catalyst which was prepared by the improved microemulsion method. There is no foreign substance except for the elements of Pt, Sn, C and O. The Pt:Sn atomic ratio is 74:26, which is very near to the nominal value of 75:25. The compositions of different Pt_xSn/C catalysts prepared by improved microemulsion method are shown in Table 1. It can be seen that all EDX compositions of Pt_xSn/C ($x = 1, 2, 2.5, 3, 4$) catalysts are quite close to the nominal values.

Fig. 3A shows TEM image of the Pt_3Sn/C catalyst. The light parts with 30–50 nm in width are the carbon support, on which there are a lot of Pt_3Sn catalysts (heavy black dots). Its high-magnification TEM micrograph is shown in Fig. 3B. It can be seen that Pt_3Sn nanoparticles prepared by improved microemulsion method are well-dispersed on the carbon support. Fig. 3C depicts the distribu-

Table 1
Composition of Pt_xSn/C catalysts prepared by improved microemulsion method.

Catalysts	Nominal composition (%)	EDX composition (%)
Pt_4Sn/C	80:20	82:18
Pt_3Sn/C	75:25	74:26
$Pt_{2.5}Sn/C$	71:29	72:28
Pt_2Sn/C	67:33	66:34
Pt_1Sn/C	50:50	51:49

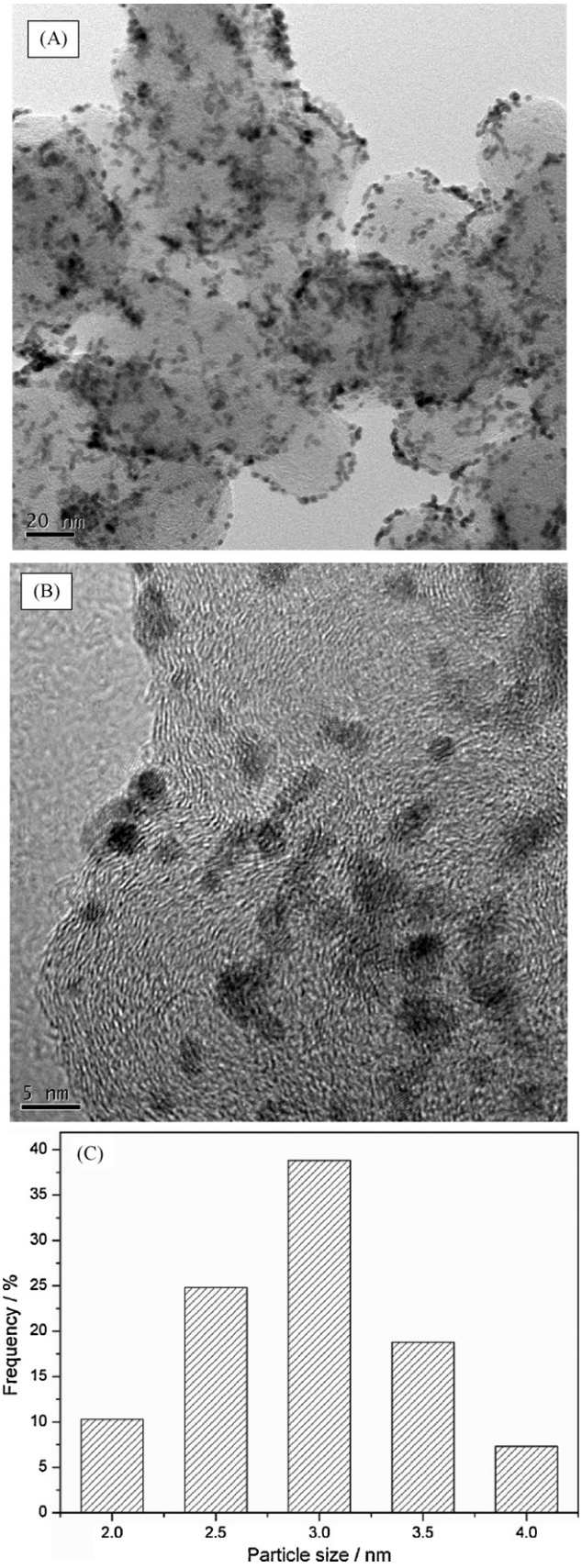

Fig. 3. (A) Low-magnification TEM micrograph of Pt_3Sn/C catalyst; (B) its high-magnification TEM micrograph; (C) its particle size distribution.

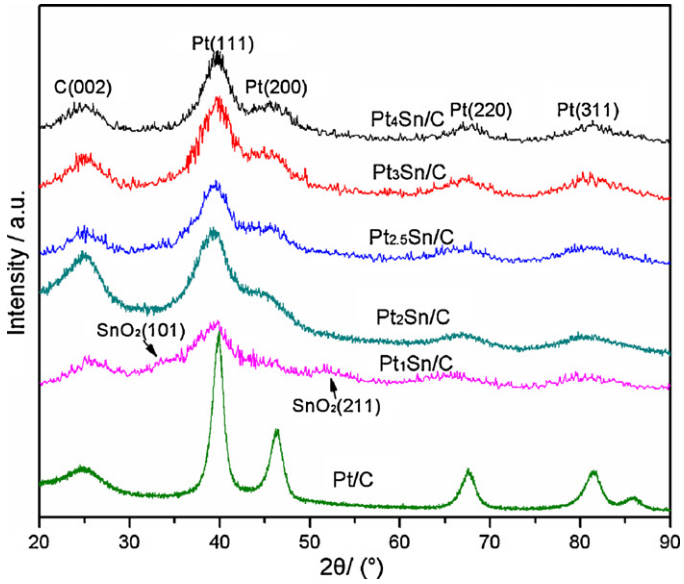

Fig. 4. XRD patterns of Pt/C (JM) and Pt_xSn/C catalysts at different Pt:Sn atomic ratios.

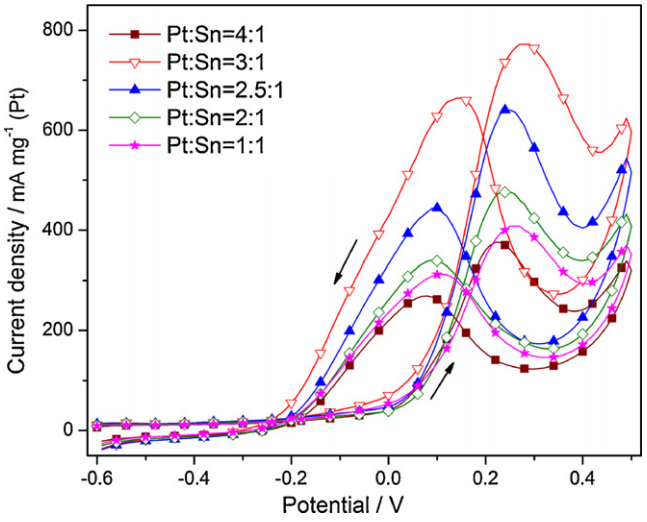

Fig. 5. Cyclic voltammograms on Pt_xSn/C catalysts with different Pt:Sn atomic ratios in 0.5 M H_2SO_4 + 1 M C_2H_5OH. Scan rate: 50 mV s^{-1}.

tion of its particle size obtained by randomly measuring particles. Seeing from Fig. 3C, the Pt_3Sn nanoparticles have a narrow size distribution in the range of 2–4 nm and its mean particle size is about 2.9 nm.

Fig. 4 shows XRD patterns of the commercial Pt/C (Johnson Matthey (JM)) and synthesized Pt_xSn/C catalysts with different atomic ratios. The diffraction peak at about 25° is corresponding to the (0 0 2) plane of the hexagonal structure of Vulcan XC-72 carbon. The diffraction peaks at around 39°, 46°, 67° and 81° are corresponding to Pt (1 1 1), (2 0 0), (2 2 0) and (3 1 1) planes, respectively. Their diffraction intensity becomes weak with the addition of Sn or the increase of the Sn:Pt ratios. And these diffraction peaks slightly shift to lower 2θ values. The shift reveals the alloying of Pt and Sn, which is caused by the incorporation of Sn in the fcc structure of Pt. The diffractogram of Pt_1Sn_1/C catalyst with the maximum Sn content also shows two weak peaks at about $2\theta = 34°$ and 52° that are corresponding to SnO_2 (1 0 1) and SnO_2 (2 1 1) planes, respectively [31]. Therefore, some of the synthesized Pt_xSn/C catalysts has part of Pt and Sn alloying. And their catalyst surface contains the multivalent tin oxides which can provide OH species and help oxidize the adsorbed intermediates resulting from ethanol oxidation [28].

3.3. Electrochemical activity of Pt_xSn/C catalysts

Fig. 5 shows the cyclic voltammograms of the ethanol oxidation on Pt_xSn/C catalysts synthesized by the improved microemulsion method. When the Pt:Sn atomic ratio is 3:1, the synthesized catalyst has the highest peak current density and the lowest onset potential. The electrochemical activity of the Pt_xSn/C catalysts for ethanol oxidation is in the order of $x = 3 > x = 2.5 > x = 2 > x = 1 > x = 4$. It indicates that the Sn in the Pt_3Sn/C catalyst has good promoting effect on the ethanol oxidation, which is in agreement with other reported results [14,36].

Since a low potential is a big concern for practical application of DEFC, the electrochemical performance of Pt_xSn/C catalysts with different Pt:Sn atomic ratios is studied by chronoamperometry at 0 V in 0.5 M H_2SO_4 + 1 M C_2H_5OH solution. Their current–time curves are shown in Fig. 6. It is found that their catalytic activity for ethanol oxidation increases greatly with the decreases of Sn content, but it becomes very low on Pt_4Sn/C catalyst. The current density on Pt_3Sn/C catalyst is much higher than that on the other catalysts. It is because the electronic conductivity of tin oxide is poor. And part of Pt active sites may be blocked by redundant Sn or its oxides if Sn content is too high, thus it will inhibit ethanol adsorption and oxidation [37]. So the addition of Sn to Pt with a suitable ratio enhances the catalytic activity for ethanol oxidation. According to the bifunctional mechanism, tin or its oxide could offer oxygen-containing species for the oxidative removal of the intermediates produced during ethanol electro-oxidation [11,38].

Fig. 7 shows the anodic linear sweep voltammograms of the ethanol oxidation on two Pt_3Sn/C catalysts and the commercial Pt/C (JM). For the Pt_3Sn/C catalyst prepared by the conventional microemulsion method (CMM), i.e. the metal precursors are dissolved in aqueous phase, its peak current density of ethanol oxidation is only 602 mA mg^{-1} (Pt), which is higher than that on the commercial Pt/C (JM) whose peak current density is 486 mA mg^{-1} (Pt). But the peak current density of ethanol oxidation on Pt_3Sn/C catalyst prepared by the improved microemulsion method (IMM) reaches 780 mA mg^{-1} (Pt). It is seen from the inset in Fig. 7 that the current density of ethanol oxidation is 41 and 33 mA mg^{-1} (Pt) on Pt_3Sn/C catalysts at −0.1 V for IMM and CMM, respectively. And

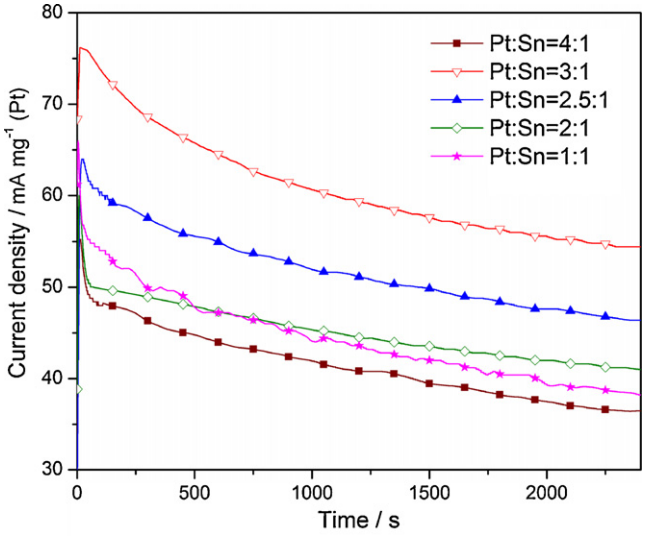

Fig. 6. Current–time curves at 0 V on Pt_xSn/C catalysts with different Pt:Sn atomic ratios in 0.5 M H_2SO_4 + 1 M C_2H_5OH.

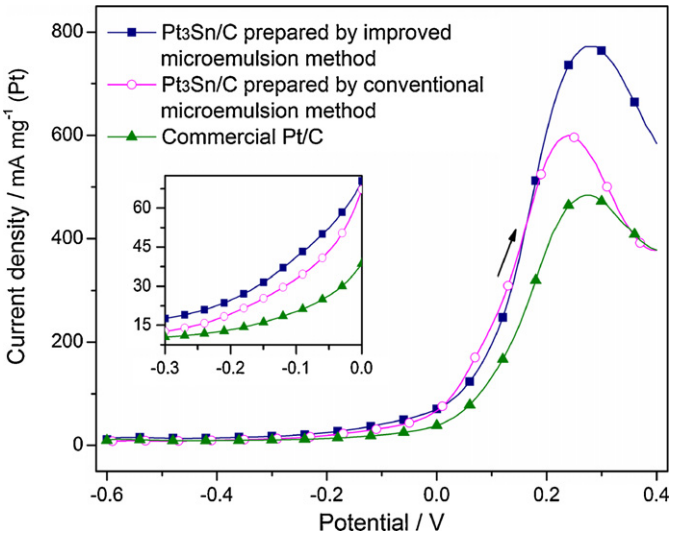

Fig. 7. Linear sweep voltammograms for ethanol oxidation on Pt_3Sn/C catalysts prepared by different microemulsion methods and on commercial Pt/C (JM) in 0.5 M H_2SO_4 + 1 M C_2H_5OH. Scan rate: 50 mV s^{-1}.

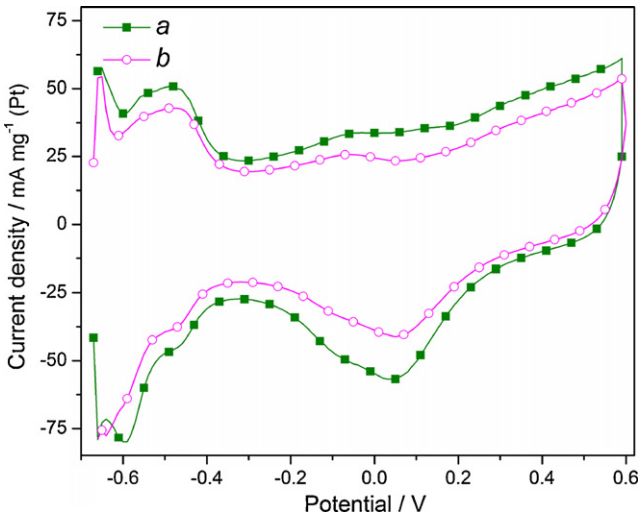

Fig. 9. Cyclic voltammograms on Pt_3Sn/C prepared by adding active carbon (*a*) before and (*b*) after precursor reduction in 0.5 M H_2SO_4. Scan rate: 50 mV s^{-1}.

it is only 20 mA mg^{-1} (Pt) on commercial Pt/C(JM) catalyst. Since the practical DEFC normally operates at the much lower potential than the peak potential of ethanol oxidation on CV, the higher current density on Pt_3Sn/C catalyst is more suitable to the practical application. Therefore, the Pt_3Sn/C catalyst prepared by IMM has much higher catalytic activity for ethanol electro-oxidation than that prepared by CMM.

The catalytic activity for ethanol electro-oxidation on Pt_3Sn/C catalysts prepared by different conditions is shown in Fig. 8. The impregnation method uses ethylene glycol as solvent and the mixture of sodium hydroxide and formic acid as reductant. The two Pt_3Sn/C catalysts synthesized by impregnation method were prepared at 90 °C and 30 °C, respectively [36]. It is seen that the forward anodic peak current density of ethanol oxidation on Pt_3Sn/C prepared by microemulsion method is 780 mA mg^{-1} (Pt), and its peak potential is 0.28 V. However, the Pt_3Sn/C catalyst synthesized by impregnation method at 90 °C has lower anodic peak current density and higher peak potential. They are 630 mA mg^{-1} (Pt) and 0.34 V, respectively. And even Pt_3Sn/C prepared by impregnation method at 30 °C has no catalytic activity

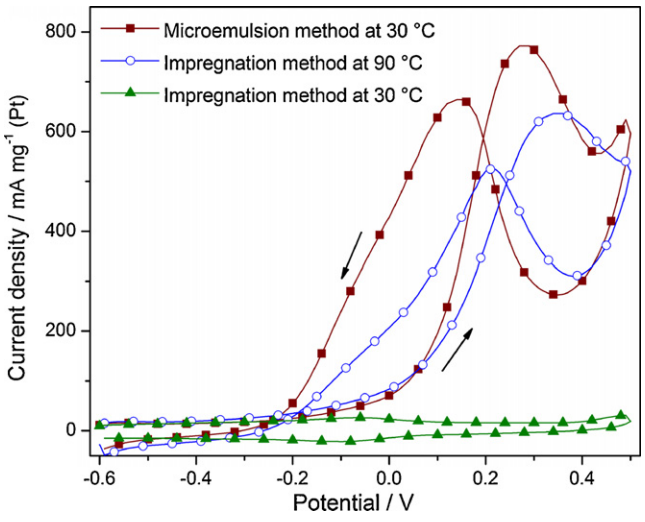

Fig. 8. Cyclic voltammograms on Pt_3Sn/C prepared by different methods in 0.5 M H_2SO_4 + 1 M C_2H_5OH. Scan rate: 50 mV s^{-1}.

for ethanol electro-oxidation. In addition, the colours of the reaction solution via impregnation method at 90 °C and improved microemulsion method at 30 °C change from yellow to colourless after separating Pt_3Sn/C catalysts, indicating the complete reduction of metal precursors. But the colour of the solution via impregnation method at 30 °C is unchanged or still yellow. It is clear that the metal precursors cannot be reduced by reductant in ethylene glycol solution at 30 °C. However, the Pt_3Sn/C prepared in microemulsion at the same temperature has a very high catalytic activity. It indicates that aqueous phase and oil phase are segmented into many "microreactors" by the molecular layer composed of surfactant and cosurfactant in microemulsion. These microreactors have very large area at the interface. On the surface of the microreactors, the metal precursors and reductant have higher reaction energy so that the reduction of metal precursors can take place even at 30 °C. The nanoparticle synthesis is also controlled by the microreactors in microemulsion.

Fig. 9 shows cyclic voltammograms of Pt_3Sn/C prepared by changing the order of adding active carbon in 0.5 M H_2SO_4 solution. The current in the range of −0.65 to −0.45 V on CV represents the adsorption and desorption of hydrogen. It is found that the specific surface area of electrochemical activity on curve *b* is lower than that on curve *a*. Fig. 10 shows the catalytic activity for ethanol electro-oxidation on these two catalysts. It is seen that the Pt_3Sn/C catalyst prepared by adding carbon before the precursor reduction (curve *a*) has much higher catalytic activity for ethanol oxidation, compared with that synthesized by adding carbon afterward (curve *b*). This behaviour is related to the adsorption of microreactors on active carbon. When the active carbon is mixed with microemulsion containing metal precursors, the microreactors in microemulsion can load on active carbon homogeneously. Then Pt_3Sn nanoparticles are deposited on the active carbon as the reductant is added. Moreover, the adsorption effects of active carbon may prevent the agglomeration of microemulsion. Finally, the nanoparticles with a narrow size distribution and a good dispersivity are obtained.

Fig. 11 shows the effect of pH value in microemulsion on the preparation of the Pt_3Sn/C catalyst. In the microemulsion of neutral system (pH = 7), the synthesized catalyst shows the highest catalytic activity for ethanol oxidation and reaches 780 mA mg^{-1} (Pt). When the pH value is changed into 2 or 12, the microemulsion shows demulsification to some extent in preparation processes so that the peak current density of ethanol oxidation decreases

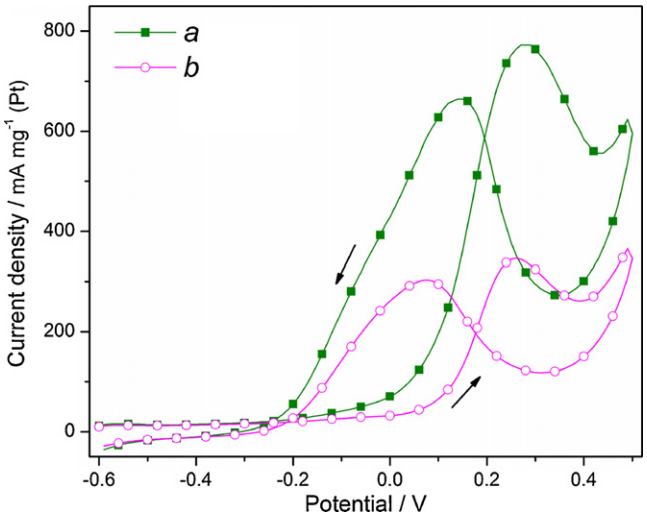

Fig. 10. Cyclic voltammograms on Pt_3Sn/C prepared by adding active carbon (*a*) before and (*b*) after precursor reduction in 0.5 M H_2SO_4 + 1 M C_2H_5OH. Scan rate: 50 mV s^{-1}.

greatly, especially in the alkaline system. It is deduced that the stability of microemulsion system is easily damaged under high or low pH values.

3.4. Pt_xSn/C nanoparticle formation in microemulsion

The schematic diagram of Pt_xSn/C nanoparticle formation in the improved preparation of microemulsion is shown in Fig. 12. Fig. 12A is a simulated diagram of the microemulsion before adding reductant, in which the surfactant (Triton X-100) and cosurfactant (ethylene glycol) form molecular layers that segment the two immiscible phases (oil/water) into many microreactors. The metal precursors are dissolved into ethylene glycol as cosurfactant. Pt^{4+} and Sn^{2+} ions exist in the form of complex in ethylene glycol even in the presence of water, which is confirmed by UV–vis spectra in Fig. 1. So the Pt–Sn complexes are present at the interface of water and oil due to the action of hydrophilic groups of ethylene glycol. Since the metal precursors at the interface have higher reaction energy, their co-reduction can occur easily at low temperature. When the reductant is added to the microemulsion, it reacts with the metal precursors with the high energy state to form the

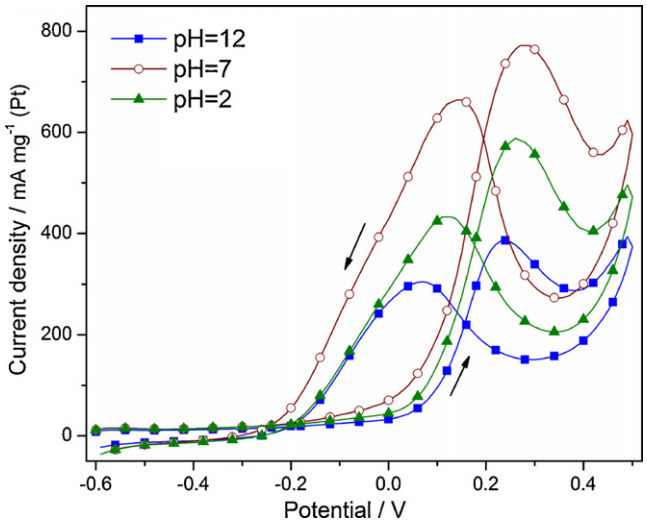

Fig. 11. Cyclic voltammograms of Pt_3Sn/C catalyst prepared in the microemulsion systems with different pH values in 0.5 M H_2SO_4 + 1 M C_2H_5OH. Scan rate: 50 mV s^{-1}.

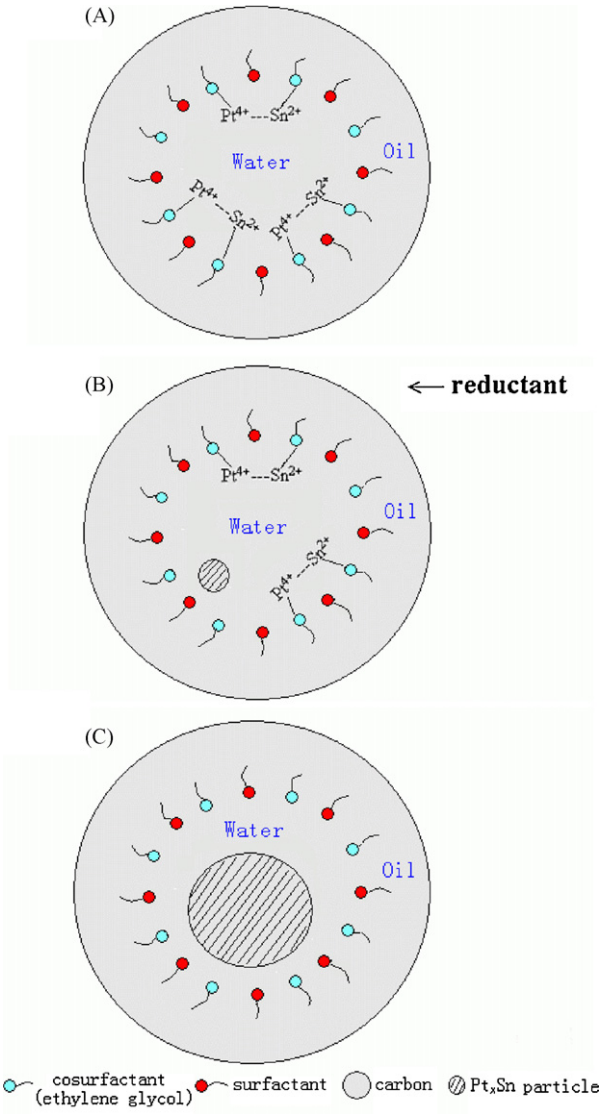

Fig. 12. Pt_xSn/C nanoparticle formation in improved microemulsion method. (A) Before adding reductant; (B) Nucleation of Pt_xSn nanoparticle; (C) Growth of nanoparticle.

nucleation of the Pt_xSn nanoparticle, which is shown in Fig. 12B. Then its growth starts at the interface and the concentration of the metal precursors decreases in the microreactors until all metal precursors are reduced completely. Fig. 12C shows the formed Pt_xSn nanoparticle. Finally, the particles deposit on active carbon. In these processes, it is beneficial to produce the Pt_xSn alloying because the reactions take place in microreactors containing the complex of Pt^{4+} and Sn^{2+}, and the microreactors can reduce the collision among particles, thus preventing the agglomeration of particles.

4. Conclusions

Pt_xSn nanoparticles (x = 1, 2, 2.5, 3, 4) supported on Vulcan XC-72R carbon for DEFC are prepared by the improved microemulsion method. In this process, the metal precursors are dissolved in ethylene glycol beforehand to prevent their hydrolysis. Pt^{4+} and Sn^{2+} ions can form a complex in ethylene glycol which acts as a cosurfactant in microemulsion. Ethylene glycol makes both metal precursors located at the water/oil interface of the microreactors and the water/oil interface has higher reaction energy. So the complex of Pt^{4+} and Sn^{2+} ions can promote their co-reduction

and alloying. And the homogenous Pt_3Sn/C particles with a narrow size distribution are obtained. Its mean nanoparticle size is about 2.9 nm. Electrochemical studies show that the Pt_3Sn/C catalyst has the highest electrochemical performance among various Pt_xSn/C ($x = 1, 2, 2.5, 3, 4$) and commercial Pt/C (JM) catalysts, and its peak current density reaches 780 mA mg^{-1} (Pt). The improved microemulsion method not only solves the problem of $SnCl_2$ hydrolysis in the water but also make Pt^{4+} and Sn^{2+} ions co-reduced and alloying of Pt and Sn to some extent. Therefore, the present microemulsion method improves the structure and behaviour of the synthesized nanocatalysts. And the Pt_3Sn/C catalyst prepared in the neutral microemulsion enhances the catalytic activity for ethanol oxidation greatly.

Acknowledgements

The authors are grateful to NSFC (No.51072037) in China and Natural Science Foundation of Fujian Province (No. 2009J01027) for financial support for this work.

References

[1] J.R.C. Salgado, F. Alcaide, G. Álvarez, L. Calvillo, M.J. Lázaro, E. Pastor, J. Power Sources 195 (2010) 4022–4029.
[2] L. Dong, R.R.S. Gari, Z. Li, M.M. Craig, S. Hou, Carbon 48 (2010) 781–787.
[3] S.S. Gupta, J. Datta, J. Electroanal. Chem. 594 (2006) 65–72.
[4] L.J. Hobson, Y. Nakano, H. Ozu, S. Hayase, J. Power Sources 104 (2002) 79–84.
[5] H.-G. Haubold, Th. Vad, H. Jungbluth, P. Hiller, Electrochim. Acta 46 (2001) 1559–1563.
[6] R.F.B. De Souza, L.S. Parreira, D.C. Rascio, J.C.M. Silva, E. Teixeira-Neto, M.L. Calegaro, E.V. Spinace, A.O. Neto, M.C. Santos, J. Power Sources 195 (2010) 1589–1593.
[7] S. Hikita, K. Yamane, Y. Nakajima, JSAE Rev. 23 (2002) 133–135.
[8] F. Colmati, E. Antolini, E.R. Gonalez, J. Electrochem. Soc. 154 (2007) B39–B47.
[9] G. Li, P.G. Pickup, Electrochim. Acta 52 (2006) 1033–1037.
[10] C. Lamy, A. Lima, V. LeRhun, F. Delime, C. Coutanceau, J.-M. Léger, J. Power Sources 105 (2002) 283–296.
[11] F. Vigier, C. Coutanceau, F. Hahn, E.M. Belgsir, C. Lamy, J. Electroanal. Chem. 563 (2004) 81–89.
[12] E. Antolini, F. Colmati, E.R. Gonzalez, J. Power Sources 193 (2009) 555–561.
[13] Z. Liu, X.Y. Ling, X. Su, J.Y. Lee, L.M. Gan, J. Power Sources 149 (2005) 1–7.
[14] L. Jiang, L. Colmenares, Z. Jusys, G.Q. Sun, R.J. Behm, Electrochim. Acta 53 (2007) 377–389.
[15] A. Oliveira Neto, M.J. Giz, J. Perez, E.A. Ticianelli, E.R. Gonzalez, J. Electrochem. Soc. 149 (2002) A272–A279.
[16] E.V. Spinacé, M. Linardi, A.O. Neto, Electrochem. Commun. 7 (2005) 365–369.
[17] S. Rousseau, C. Coutanceau, C. Lamy, J.-M. Léger, J. Power Sources 158 (2006) 18–24.
[18] E.V. Spinacé, R.R. Dias, M. Brandalise, M. Linardi, A.O. Neto, Ionics 16 (2010) 91–95.
[19] E. Antolini, J. Power Sources 170 (2007) 1–12.
[20] S.Q. Song, W.J. Zhou, Z.H. Zhou, L.H. Jiang, G.Q. Sun, Q. Xin, V. Leontidis, S. Kontou, P. Tsiakaras, Int. J. Hydrogen Energy 30 (2005) 995–1001.
[21] W. Zhou, Z. Zhou, S. Song, W. Li, G. Sun, P. Tsiakaras, Q. Xin, Appl. Catal. B: Environ. 46 (2003) 273–285.
[22] W.J. Zhou, B. Zhou, W.Z. Li, Z.H. Zhou, S.Q. Song, G.Q. Sun, Q. Xin, S. Douvartzides, M. Goula, P. Tsiakaras, J. Power Sources 126 (2004) 16–22.
[23] H. Li, G. Sun, L. Cao, L. Jiang, Q. Xin, Electrochim. Acta 52 (2007) 6622–6629.
[24] S. García-Rodríguez, M.A. Peña, J.L.G. Fierro, S. Rojas, J. Power Sources 195 (2010) 5564–5572.
[25] W.-Z. Hung, W.-H. Chung, D.-S. Tsai, D.P. Wilkinson, Y.-S. Huang, Electrochim. Acta 55 (2010) 2116–2122.
[26] S. García-Rodríguez, F. Somodi, I. Borbáth, J.L. Margitfalvi, M.A. Peña, J.L.G. Fierro, S. Rojas, Appl. Catal. B: Environ. 91 (2009) 83–91.
[27] G. Siné, G. Fóti, Ch. Comninellis, J. Electroanal. Chem. 595 (2006) 115–124.
[28] M. Zhu, G. Sun, Q. Xin, Electrochim. Acta 54 (2009) 1511–1518.
[29] F. Colmati, E. Antolini, E.R. Gonzalez, Appl. Catal. B: Environ. 73 (2007) 106–115.
[30] D.R. Lycke, E.L. Gyenge, Electrochim. Acta 52 (2007) 4287–4298.
[31] Z. Liu, B. Guo, L. Hong, T.H. Lim, Electrochem. Commun. 8 (2006) 83–90.
[32] M. Boutonnet, J. Kizling, P. Stenius, G. Maire, Colloids Surf. 5 (1982) 209–225.
[33] L. Xiong, A. Manthiram, Electrochim. Acta 50 (2005) 2323–2329.
[34] T. Teranishi, M. Hosoe, T. Tanaka, M. Miyake, J. Phys. Chem. B 103 (1999) 3818–3827.
[35] L. Jiang, G. Sun, Z. Zhou, W. Zhou, Q. Xin, Catal. Today 93–95 (2004) 665–670.
[36] Y. Guo, Y. Zheng, M. Huang, Electrochim. Acta 53 (2008) 3102–3108.
[37] W.J. Zhou, S.Q. Song, W.Z. Li, Z.H. Zhou, G.Q. Sun, Q. Xin, S. Douvartzides, P. Tsiakaras, J. Power Sources 140 (2005) 50–58.
[38] L. Jiang, G. Sun, S. Sun, J. Liu, S. Tang, H. Li, B. Zhou, Q. Xin, Electrochim. Acta 50 (2005) 5384–5389.